Published in The Journal of Chemical Physics 124, 054717 (11 pages), 2006
which should be used for any reference to this work

Simultaneous *in situ* monitoring of surface and gas species and surface properties by modulation excitation polarization-modulation infrared reflection-absorption spectroscopy: CO oxidation over Pt film

Atsushi Urakawa
Department of Chemistry and Applied Biosciences, ETH Zurich, CH-8093 Zürich, Switzerland

Thomas Bürgi[a)]
Institut de Chimie, Faculté des Sciences, Université de Neuchâtel, Rue Emile-Argand 11, CH-2007 Neuchâtel, Switzerland

Hans-Peter Schläpfer and Alfons Baiker[b)]
Department of Chemistry and Applied Biosciences, ETH Zurich, CH-8093 Zürich, Switzerland

A method for *in situ* monitoring of surface and gas species utilizing separately the difference and sum reflectivity of two polarizations, normal and parallel to the surface, measured by polarization-modulation infrared reflection-absorption spectroscopy is presented. Surface and gas-phase spectra were separately but simultaneously obtained from the reflectivities. The technique is combined with modulation excitation spectroscopy to further enhance the sensitivity, and a small-volume cell was designed for this purpose. CO oxidation over a 40 nm Pt film on aluminum was investigated under moderate pressure (atmospheric pressure, 5% CO, and 5%–40% O_2) at 373–433 K. The surface species involved in the oxidation process and the gas-phase species, both reactant (CO) and product (CO_2), could be simultaneously monitored and analyzed quantitatively. In addition, the reflectivity change of the sample during the reaction was assigned to a near-surface bulk property change, that is, surface reconstruction to the oxide phase. Under an O_2-rich atmosphere, two reactive phases, denoted as low- and high-activity phases, were identified. A large amount of atop CO was observed during the low-activity phase, while the adsorbed CO completely disappeared during the high-activity phase. The presence of an infrared-inactive CO_2 precursor formed by the reaction between surface oxide and gaseous CO during the high-activity phase was inferred. The desorption of the CO_2 precursor is facilitated under a CO-rich atmosphere, most likely, by surface reconstruction to metallic Pt and a competitive adsorption of CO on the surface.

I. INTRODUCTION

After the pioneering experimental and theoretical works by researchers in the 1950s and the 1960s[1] infrared reflection-absorption spectroscopy, often noted as IRRAS, IRAS, or RAIRS, has been recognized as one of the most sensitive methods in surface analysis, e.g., for the study of surface structures, chemical states of adsorbates, and their interactions.[2] The so-called surface selection rule allows one to extract information about the orientation of surface species.[3] The use of a photoelastic modulator[4] (PEM) further enhances the sensitivity of IRRAS considerably and a surface spectrum can be measured within a short time compared with conventional IRRAS. Another important advantage of the polarization-modulation infrared reflection-absorption spectroscopy (PM-IRRAS) method is the cancellation of the bulk phase absorption (here "bulk" is defined as the phase where light is radiated from and reflected out at the interface) due to the differential nature of the measurement.[5] This allows the investigation of surface structures and species residing at the gas-solid,[6,7] gas-liquid,[8] and even liquid-solid interfaces.[9] In IRRAS and PM-IRRAS, the surface spectra are obtained as a differential reflectivity, and, in principle, it is possible to obtain the absorbance of species in a bulk phase from the reflectivities, being not only used for compensation of bulk phase absorbances in surface spectrum calculation. To our knowledge, there is only one work reported in the literature that has made use of the bulk absorbance information obtained during IRRAS measurements.[10] The PM-IRRAS method, with its surface sensitivity, relatively high time resolution, and the possibility to follow simultaneously the time evolution of bulk species, will certainly enhance our knowledge on surface processes, as a rather complete picture (including surface species and bulk phase) can be obtained.

CO oxidation over platinum is one of the most intensively studied fields in heterogeneous catalysis, initiated by the pioneering work of Langmuir.[11] The apparent simplicity of the reaction and its relevance in combustion and automobile-exhaust catalysis and phenomena of general interest such as oscillation in reaction rate, render CO oxidation still an active research field.[12] Recent research aiming at

[a)]Electronic mail: thomas.burgi@unine.ch
[b)]Electronic mail: baiker@chem.ethz.ch

bridging the pressure gap revealed large differences in the behavior under UHV and industrially relevant conditions, indicating the absolute necessity of surface studies under high pressures.[7,13] In particular, for CO oxidation over Pt, under a relatively high oxygen pressure (0.5 bar), very active Pt-oxide islands are observed by scanning tunneling microscopy (STM).[14] The oscillatory behavior of the reaction is also explained by metal-oxide islands formation,[15] which was never observed under UHV conditions.[16] Bridging the pressure gap by theoretical means was also attempted and the higher reactivity of such an oxide phase compared with that of a Pt surface was shown.[17] Various surface-sensitive techniques have been used under UHV conditions,[18–22] but only a few techniques could be applied under relatively high pressures. Among surface-sensitive vibrational spectroscopies, IRRAS has been used to study CO oxidation over Pt at low pressures[23–26] except one study under a high oxygen pressure (ca. 0.5 bar).[10] Sum frequency generation (SFG) has been applied to study the same reaction system under UHV as well as high pressure. The nature of the active species and the effects of CO dissociation on the activity under high pressures and temperatures below and above the ignition temperature, at which the reaction becomes self-sustained, have been investigated.[27] Through these studies many aspects concerning surface species and properties under technically more relevant conditions became available, yet obviously there is a need for further methods allowing detection of both surface and bulk phase species with a high time resolution under realistic conditions to gain new insights into the reaction system.

In this work, a method facilitating simultaneous monitoring of surface and gas-phase species is presented that utilizes the absorbances contained in the two reflected beams of different polarizations. Modulation excitation spectroscopy[28,29] (MES) is combined with the method to further enhance the signal-to-noise ratio and obtain kinetic information of surface species. A small-volume cell was designed to allow fast exchange of the atmosphere above the surface. The sensitivity and power of the technique, modulation excitation polarization-modulation infrared reflection-absorption spectroscopy (ME PM-IRRAS), are demonstrated by CO oxidation over a 40 nm Pt film deposited on Al.

II. EXPERIMENT

A. Preparation of Pt thin film

Pt films were used to study CO oxidation. Although a Pt(111) crystal was used to demonstrate the feasibility of the technique during CO adsorption/desorption, the application of a film allowed higher reproducibility by simply exchanging the sample after surface contamination affected the measurements. A square aluminum plate ($10\times10\times1$ mm) was coated with 40 nm Pt by physical vapor deposition with a Balzers BAE-370 vacuum coating system at room temperature, which ensures the complete covering of the aluminum. Pt was heated in a graphite crucible by means of an electron beam at a pressure of about 1.5×10^{-5} mbar. A quartz crystal sensor was used to measure the mass thickness of the films.

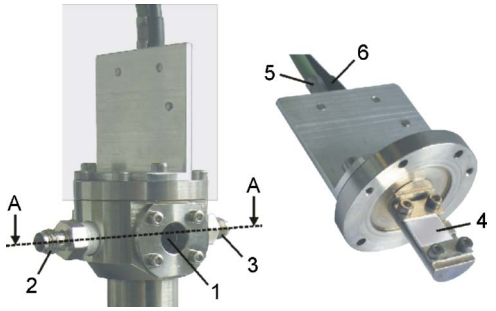

FIG. 1. (Left) view of the entire ME PM-IRRAS cell. (Right, opaque region of the left) sample holder attachment with heating system. (1) BaF_2 window, (2) gas inlet, (3) gas outlet, (4) sample, (5) thermocouple, and (6) heating element.

The deposition rate was 0.05 nm s^{-1}. The distance between the evaporation source and the Al plate was about 33 cm, yielding even films over the entire plate.

B. Design of the ME PM-IRRAS cell

A small-volume cell for ME PM-IRRAS with a short light path length was designed and built (Fig. 1).[30] A small volume is necessary for fast exchange of gases, and a short path length is desirable to achieve excellent compensation of the gas phase in the PM-IRRAS surface spectrum by minimizing absorption due to gas-phase species against surface ones. The inner cell volume was estimated to be ca. 6.9 ml (the number can differ slightly due to the volume of screws of the sample holder). The path length (window-sample-window) is 25.9 mm and the distance between the gas inlet and the sample surface is 7 mm. In order to enhance the homogeneity of the gas supply over a sample surface and a better gas exchange within the cell, the gas inlet consists of five holes (each 0.7 mm in diameter) targeting the four edges of the sample and the center.[30] Samples can be heated to 623 K, and the temperature is measured by means of a thermocouple inside the sample holder. The gas-mixing behavior of the cell under various flow rates and modulation frequencies was studied by the gas-phase information contained in the ME PM-IRRAS spectra and will be reported elsewhere.[31]

C. Modulation excitation spectroscopy

MES, more precisely the detection method, phase sensitive detection (PSD), is a powerful technique to significantly enhance the signal-to-noise ratio and extract kinetic information of reversible systems. The technique has been applied successfully in the study of chemical and physical systems, for example, heterogeneous catalysis,[28] chiral interaction,[32] biological interaction,[33] and diffusion.[34]

If a system is perturbed by varying an external parameter (e.g., temperature, concentration, light flux, *p*H) periodically, all the species in the system, which are affected by this parameter, will also be affected periodically at the same frequency as the stimulation (ω) or harmonics thereof.[29] It is possible that there is a phase lag between excitation and response, which contains information about the kinetics of the species in the system. At the beginning of the modulation the system relaxes to a new quasi-steady-state around which it is

oscillating at a frequency ω. In this quasi-steady-state, the absorbance variations $A(\tilde{\nu},t)$ are followed by measuring spectra at different times within the modulation period T. This set of spectra, the time-domain absorbance spectra $A(\tilde{\nu},t)$, is then converted into phase-domain absorbance spectra $A(\tilde{\nu},\phi^{\mathrm{PSD}})$ by a mathematical treatment, the so-called PSD or demodulation, according to

$$A_k(\tilde{\nu},\phi_k^{\mathrm{PSD}}) = \frac{2}{T}\int_0^T A(\tilde{\nu},t)\cdot\sin(k\omega t+\phi_k^{\mathrm{PSD}})dt. \quad (1)$$

The integer variable k determines the frequency at which the time-dependent signals are demodulated, that is, the fundamental of the excitation frequency ($k=1$), first harmonic ($k=2$), and so on. In this study, the fundamental demodulation ($k=1$) was analyzed.

D. ME PM-IRRAS and data acquisition

The sample was mounted in the cell located within the compartment of a Bruker PMA 37 connected to the external beam port of a Bruker vector 33 Fourier transform infrared spectrometer. The angle of incidence was 80° and the light was focused on a liquid nitrogen-cooled MCT detector. Polarization was modulated at a frequency of 50 kHz with a PEM (Hinds Instruments, PEM-90, ZnSe modulator optical head) set for half-wave retardation at 1800 cm^{-1}. Demodulation was performed with a lock-in amplifier (Stanford Research Systems, SR830 DSP). In order to enhance the signal-to-noise ratio, an optical low-pass filter ($<4000\ \mathrm{cm}^{-1}$) was put before the PEM. All spectra were recorded at 4 cm^{-1} resolution. 60 ml/min of 5% CO (4.7, Messer Griesheim GmbH) in the first-half period and 5%–40% O_2 (5.0, PanGas) in the second-half period, both balanced with He (5.0, PanGas), were alternately flowed into the cell. Sixty spectra were recorded per modulation period T. Signal averaging was performed over 3, 5, 10, and 20 periods after 1, 1, 2, and 4 initial periods to reach quasi-steady-states, and each of the 60 spectra in a period was obtained from 16, 8, 4, and 2 scans at the modulation frequency of 0.97, 1.94, 3.88, and 7.76 mHz ($T=1032.7, 516.1, 257.9, 128.8$ s), respectively. Prior to the experiments, samples were heated to the measurement temperature and kept under 40% O_2 in He until adsorbed CO from previous experiments was completely removed.

E. Data processing and analysis

A PM-IRRAS spectrum is, in principle, measured taking the ratio of ΔR [$|R_p-R_s|$, the reflectance difference of p (parallel to the plane of incident light) and s (perpendicular to the plane of incident light) component] and R (R_p+R_s, the sum of the reflectances),

$$\frac{\Delta R}{R} = \frac{|R_p-R_s|}{R_p+R_s}. \quad (2)$$

In reality, the differential and sum spectra are more complicated due to the PEM used to modulate the polarization, optical components located in the setup, and sensitivity enhancement by the lock-in amplifier. The more precise expression of the experimental PM-IRRAS spectrum is given by[35,36]

$$\frac{\Delta R}{R} = \frac{g\cdot|(\gamma R_p-R_s)\cdot J_2(\varphi_0)|}{(\gamma R_p+R_s)\pm(\gamma R_p-R_s)\cdot J_0(\varphi_0)}, \quad (3)$$

where g is a constant accounting for the different gain and filtering occurring during the two-channel electronic processing; $\gamma(=C_p/C_s)$ is a factor taking the polarization effects by the optoelectronic components into account, where C_p and C_s are different overall responses of the optoelectronic setup for the p and s polarizations; and $J_0(\varphi_0)$ and $J_2(\varphi_0)$ are zero- and second-order Bessel functions of the maximum dephasing φ_0 introduced by the PEM. The plus and minus signs in the equation correspond to the cases where p or s polarization is used before the PEM, respectively (here s polarization was used).

The basic idea of the current work is to take advantage of the reflectance difference [the numerator in Eq. (3)], which contains surface information, and the sum reflectance [the denominator in Eq. (3)], which contains gas-phase information, separately. They are obtained simultaneously through different channels during measurements. The numerator can be written as $|(R_p-R_s)\cdot J_2(\varphi_0)|$ after the gain is properly taken into account and when $\gamma=1$. Clearly, the numerator is the *difference* in the reflectivity between the p and s polarizations of the samples, and therefore it contains information about surface species due to the surface selection rule. On the other hand, the denominator can be approximately written as R_p+R_s when $\gamma=1$, if the sample is highly reflective (such as for a metal, $R_p\simeq R_s$). General PM-IRRAS experiments utilize R_p+R_s only to compensate for gas-phase contributions in the surface spectrum [i.e., $|(R_p-R_s)\cdot J_2(\varphi_0)|$]. R_p+R_s contains enhanced absorption of the surface species but also gas-phase information when IR-absorbing gases are present inside and outside the cell. The absorbance of surface species are negligible in our setup (up to a few percent) compared with one of the gas-phase species, and therefore R_p+R_s can approximately be considered as a single-beam spectrum of the gas phase. When necessary, it is possible to remove the contributions of surface species by calibrating correctly the setup and calculating the Bessel functions.[35]

In this work the PM-IRRAS spectra are normalized by the last spectrum of the 60 spectra of a period, which yields excellent compensation of background (e.g., the Bessel functions and the optoelectronic components). This was possible because the last spectrum during the CO/O_2 modulation experiments contained nearly no visible signals in the mid-IR under the conditions used in this study.

Hence, the normalized PM-IRRAS spectrum is obtained as

$$\left(\frac{\Delta R}{R}\right)_{\mathrm{norm}} = \frac{(\Delta R/R)}{(\Delta R/R)_{\mathrm{last}}} - 1. \quad (4)$$

F. CO adsorption on Pt(111)

In order to demonstrate the sensitivity of the method for both surface and gas-phase spectra, CO adsorption on a Pt(111) single crystal was studied by modulating 60 ml/min

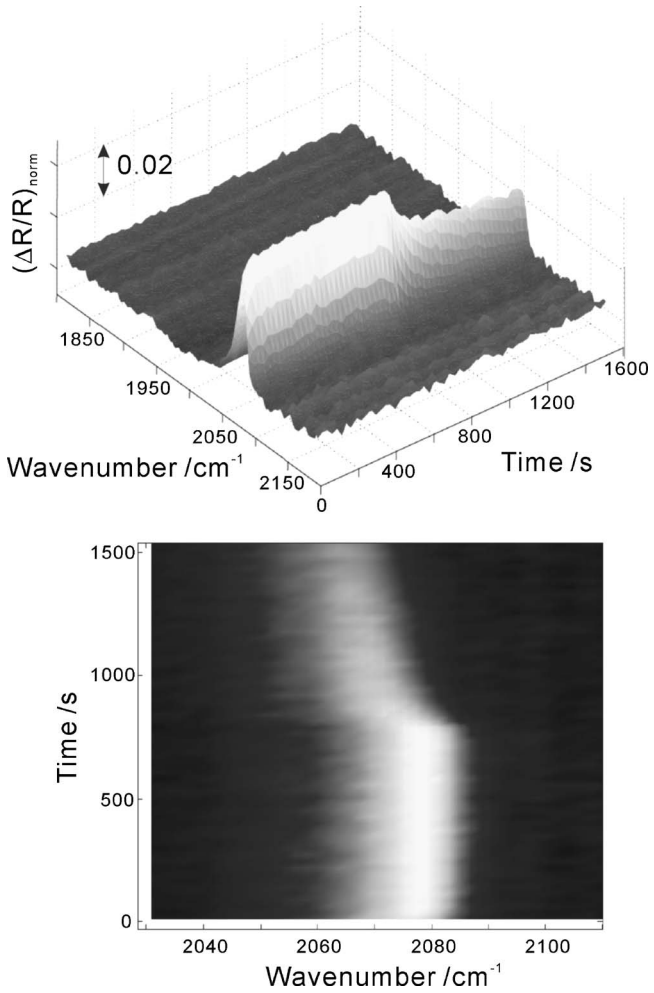

FIG. 2. Normalized ME PM-IRRAS surface spectra of adsorbed CO on Pt(111) at 423 K (top: 3D plot, bottom: top view of top figure). First-half period: 5% CO in He, second-half period: He, both 60 ml/min, T =1549.2 s. The sampling (60 data points per period and 24 scans for each) and averaging were performed over two periods after one initial period. The spectra were normalized by the spectra obtained after heating pretreatment at 573 K under He prior to the ME experiment.

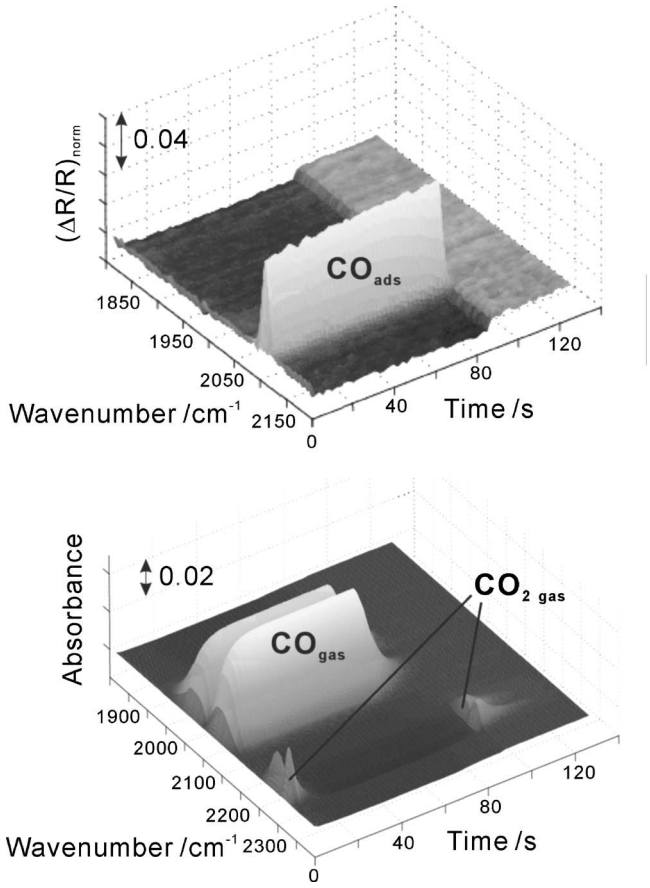

FIG. 3. ME PM-IRRAS surface (top) and gas-phase (bottom) spectra of CO and CO_2 stretching frequency region. First-half period: 5% CO in He, second-half period: 40% O_2 in He, both 60 ml/min, T=128.8 s at 433 K. For normalization and absorbance calculations the last spectrum of the time series was used.

of 5% CO in He and He at 423 K. The Pt(111) single crystal was cleaned by Ar^+ sputtering, mounted in the setup, and annealed at 573 K. No signals were observed after that in the PM-IRRAS; however, the pretreatment at low temperature likely does not lead to the complete annealing of the surface. Figure 2 shows the PM-IRRAS surface spectra and the PM-IRRAS gas-phase spectra are shown in the supporting information.[30] It should be emphasized that the surface and gas-phase spectra were obtained *simultaneously* in a single measurement. A clear adsorbed atop CO band at 2078 cm^{-1} and the slow desorption of CO with a gradual redshift to 2064 cm^{-1} was observed in the surface spectra (Fig. 2). The compensation of the gas-phase contributions was excellent. Experiments with longer periods (up to 2324 s) and at higher temperatures (up to 453 K) showed no complete desorption of CO from the Pt surface. No bridge-bonded CO near 1850 cm^{-1} was observed. The gas-phase spectra were obtained with a better signal-to-noise ratio and it showed only gaseous CO bands in the first-half period and no detectable species in the second-half period.[30]

III. RESULTS

A. CO oxidation over Pt film

PM-IRRAS surface and gas-phase spectra of a CO/O_2 modulation experiment (first-half period: 5% CO in He, second-half period: 40% O_2 in He, both 60 ml/min; modulation frequency of 7.76 mHz at 433 K) are shown in Fig. 3. In the surface spectra, an adsorbed atop CO band was clearly observed at 2100 cm^{-1}; however, in contrast to the CO/He modulation experiment (Fig. 2) the adsorbed CO band completely and sharply disappeared (ca. 20 s) after the valve was switched to oxygen, accompanied by a homogeneous broadband step increase of the baseline. In contrast, when the valve was switched to CO, a sharp increase in the adsorbed CO band was observed, accompanying a step decrease of the baseline. The same behavior was also observed for Pt(111), and the baseline step change under different conditions [Pt(111) and Pt film at different temperatures] was between 0.002 and 0.01 [in normalized IRRAS units, Eq. (4)]. Possible causes for the baseline change will be discussed later. The CO adsorption was very fast compared with the stimulation, i.e., the concentration change of CO gas in the cell.

Furthermore, the oxidation product, CO_2 gas, could be detected with this setup (Fig. 3, bottom). CO_2 was formed when the valve was switched to CO and also when the ad-

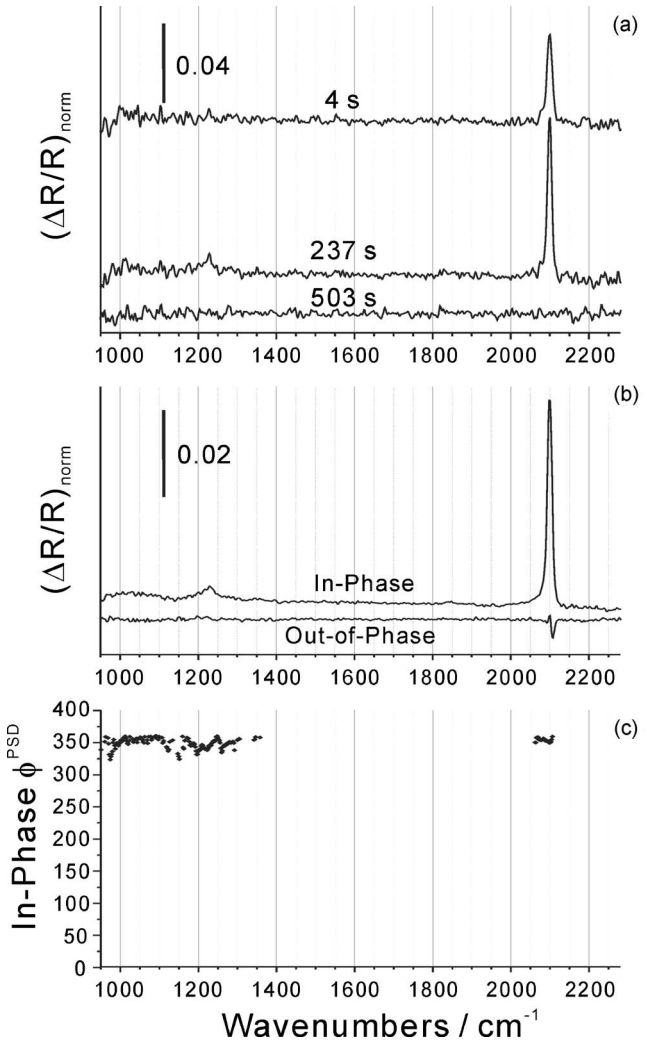

FIG. 4. (a) Selected time-domain spectra at different times during the modulation period, (b) in-phase (ϕ^{PSD}=349°) and out-of-phase (ϕ^{PSD}=259°) phase-domain spectra, and (c) in-phase angles of the phase-domain spectra. First-half period: 5% CO in He, second-half period: 40% O_2 in He, both 60 ml/min, T=516.1 s at 433 K. For (c), the angles at which the in-phase amplitude values are above a cutoff of 0.001 (normalized IRRAS unit) are shown.

sorbed CO band disappeared under O_2 atmosphere. The reasons for this behavior of CO_2 formation was examined in detail with experiments using various O_2 concentrations, modulation periods, and temperatures, as will be discussed later.

Figures 4(a) and 4(b) show selected time-domain and phase-domain spectra of a CO/O_2 modulation experiment at 3.88 mHz (except for the modulation frequency, the conditions are the same as above). Prior to demodulation, the baseline of the time-domain spectra was corrected. As seen in Fig. 3 (top) and also considering Eq. (1), the amplitude step change of the baseline will also appear in the phase-domain spectra, and the contribution should be minimized in order to maximize the amplitudes of surface species bands. Here the baseline was corrected by subtracting the average value between 1600 and 1700 cm^{-1} to minimize the effect. Figure 4(a) shows three time-domain spectra at different times of a period. The spectra were noisy, which makes it difficult to analyze surface species except for adsorbed CO.

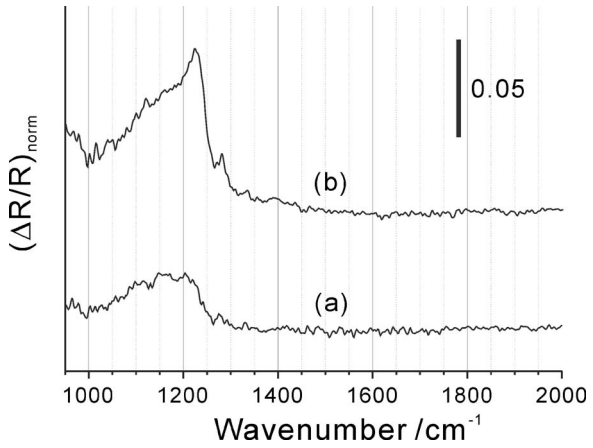

FIG. 5. PM-IRRAS spectra of surface species formed during the experiments. (a) after ca. 6 h of CO/O_2 modulation experiments at 403 K. (b) after a total ca. 18 h of CO/O_2 modulation experiments at 373, 403, and 433 K.

On the other hand, the phase-domain spectra improved the signal-to-noise ratio significantly [Fig. 4(b)] and allowed confidently assigning the surface species dynamically formed by the concentration modulation. In the phase-domain spectra, the adsorbed CO band (2100 cm^{-1}) and two other bands (1050 and 1230 cm^{-1}) were observed. The out-of-phase spectrum is almost a straight line, except for the small dispersive band near 2100 cm^{-1}. This is due to the small frequency shift of the adsorbed CO band upon CO adsorption and disappearance by desorption or reaction. The in-phase angles in Fig. 4(c), containing information about the kinetics of the process, are the same for all the bands at each frequency, implying the same time-response behavior of the surface species causing the bands. Figure 5 shows two PM-IRRAS spectra recorded after the modulation experiments. The surface species at 1050 and 1230 cm^{-1}, observed in the in-phase phase-domain spectrum [Fig. 4(b)], responded in the same manner as the adsorbed CO and furthermore accumulated during the experiments. It should be noted that periodically accumulating species (stair function) also appear in a phase-domain spectrum. The broad band (950–1300 cm^{-1}) gradually increased with increasing number of experiments (Fig. 5).

B. Effects of oxygen concentration

The effect of oxygen concentration on CO oxidation over Pt film was studied by modulating 5% CO (the first-half period) and 5%, 10%, 20%, and 40% O_2 (the second-half period) in He at the modulation frequency of 7.76 mHz (T =128.8 s). The responses of the adsorbed CO and the formed CO_2 gas are shown in Figs. 6(b) and 6(c) in comparison to the response of CO gas stimulation [Fig. 6(a)]. A similar CO adsorption level was found for all the conditions. There were delays in the disappearance of the adsorbed CO [Fig. 6(b)] as is also evident from Fig. 3. The delay increased when the oxygen concentration decreased. In all experiments using the different oxygen concentrations, similar baseline step changes were observed upon the adsorbed CO disappearance. CO_2 gas was formed when the adsorbed CO band dis-

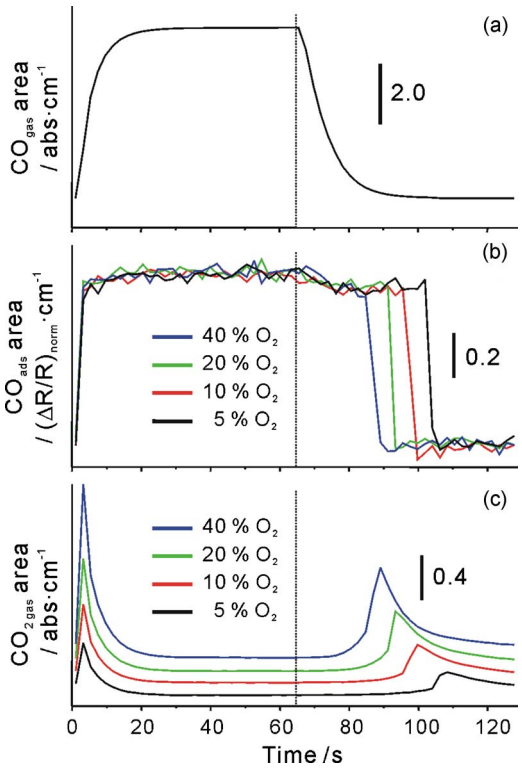

FIG. 6. Concentration profiles of surface/gas species during CO/O_2 modulation experiments over Pt film with different O_2 concentrations (5%–40%) at 433 K. (a) CO gas, (b) adsorbed CO, (c) CO_2 gas. First-half period: 5% CO in He, second-half period: 5%–40% O_2 in He, both 60 ml/min, T =128.8 s. The dotted line in the middle indicates the end of the first-half period (the beginning of the second-half period).

appeared and also when the gas was switched to CO as described previously. The amount of CO_2 formation expressed by the integrated area of CO_2 gas signal at different oxygen concentrations [Fig. 6(c)] is shown in Fig. 7. A clear monotonous-increase relation between the oxygen concentration and the amount of CO_2 gas formed was found.

C. Effects of temperature

Furthermore, the effect of temperature on the CO_2 gas formation was studied. Figure 8 shows the amount of CO_2 gas formed at three different temperatures (373, 403, and 433 K) and four different modulation frequencies. An increase in the CO_2 gas formation at the longer modulation

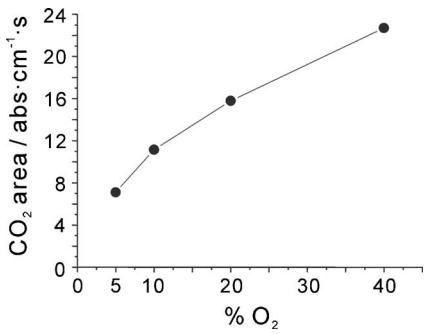

FIG. 7. Amount of CO_2 formation during CO/O_2 modulation experiments over Pt film with different O_2 concentrations (5% CO and 5%–40% O_2 in He, T=128.8 s at 433 K).

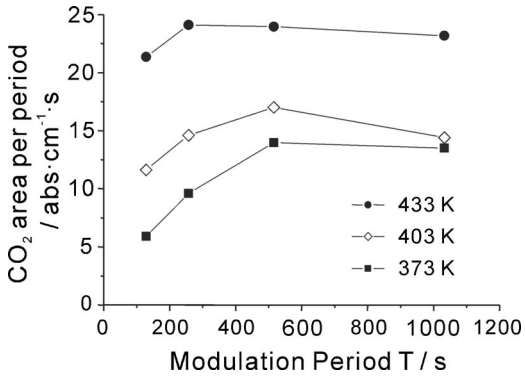

FIG. 8. Amount of CO_2 formation during one modulation period over Pt film at different temperatures [5% CO (first-half period) and 5%–40% CO (second-half period) in He, modulation periods: 128.8, 257.9, 516.1, and 1032.7 s, at 373, 403, and 433 K].

period was observed at 373 and 403 K; however, nearly constant CO_2 gas formation was observed at 433 K. Figure 9 shows the amounts of CO_2 gas during a modulation period measured using different modulation frequencies at 433 K. It should be noted that the integrated areas measured at the different modulation frequencies are nearly constant at 433 K (Fig. 8). When the modulation period is long, for example, at T=1032.7 s, the second CO_2 gas formation (when the adsorbed CO disappears in O_2 atmosphere) is significantly more prominent than the first CO_2 gas formation (when the gas is switched from O_2 to CO). However, as the period becomes shorter, for example, at T=128.8 s, the first and second CO_2 forms are similar. A sharper formation peak was observed for the first CO_2 formation. Another interesting observation is the long tail of CO_2 in O_2 atmosphere. For instance, the CO_2 formation level does not reach zero during the second-half period at T=128.8 s. The time- and phase-domain PM-IRRAS spectra measured at different temperatures showed similar bands as in Fig. 4 (not shown here). Furthermore, the adsorbed CO bands were broader and slightly redshifted at lower temperatures (centered at 2108 cm^{-1} at 373 K and at 2100 cm^{-1} at 433 K), although the adsorption amounts judged from the integrated area at different temperatures were nearly equal.

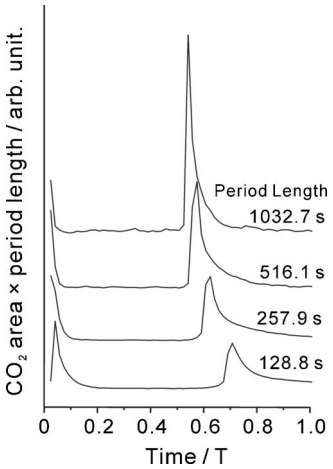

FIG. 9. CO_2 formation behavior at different modulation frequencies (T =128.8, 257.9, 516.1, and 1032.7 s). Time is shown relative to the modulation periods.

IV. DISCUSSION

A. Modulation excitation PM-IRRAS

A technique to simultaneously monitor gas and surface species utilizing surface parallel and normal polarizations has been developed and combined with the modulation excitation (ME) technique to further enhance sensitivity and allow kinetic studies. The capability has been demonstrated by a quantitative study of CO adsorption and oxidation on Pt. It showed excellent sensitivity in detecting surface species at monolayer coverage under pressure. The simultaneous monitoring can provide insight on the phenomena occurring at the gas-solid interface. Furthermore, baseline move of ME PM-IRRAS surface spectra contains the change of the surface property as discussed later.

B. CO on Pt

CO vibrational frequency shifts were observed upon temperature and atmosphere changes, which indicate the influence of the surface and surrounding on the adsorbed molecules. Figure 2 shows the redshift during the atop CO desorption. This redshift agrees well with the previous SFG studies[37,38] and also with the IRRAS study of the CO-coverage-dependent frequency shift.[39] The origin of the higher frequency has been assigned to the enhancement of dipole coupling between CO molecules at high coverage, i.e., at higher density, which weakens the CO–Pt interaction.[39] Bridge-bonded CO was not found during our measurements. This observation is supported by the fact that the bridge-bonded CO is only observable at UHV conditions and only atop CO is found at pressures above ca. 1.3 mbar.[37]

Furthermore, the atop CO stretching frequency was higher by 10 cm^{-1} during the CO/O_2 experiments than during the CO/He experiments over Pt film [and also the Pt(111) single crystal] at the same temperature (not shown here). A similar frequency shift was observed by IRRAS for CO on oxygen-precovered Pt,[25] which proves the presence of oxygen on the Pt surface near the adsorbed CO during the CO/O_2 modulation experiments. There was almost no CO frequency shift during the sudden disappearance of adsorbed CO in the CO/O_2 modulation experiment (Fig. 3). This indicates that the movement of CO is more confined on the surface due to the presence of oxygen; however, this disappearance of the adsorbed CO is most probably *not* due to a simple desorption of CO from the Pt surface and must be carefully examined. This point will be discussed further in the next section. Also, no bridge-bonded CO was found during the CO/O_2 modulation experiments. This may be related to the observations made by IRRAS (Ref. 25) and electron energy loss spectroscopy[40] (EELS) that there was no bridge-bonded CO on more than a quarter monolayer of oxygen-precovered Pt surface.

C. CO oxidation over Pt

1. Reaction mechanism and possible surface species

a. CO_2 formation mechanism under CO and O_2 atmospheres. CO_2 formation was observed twice during a CO/O_2 modulation cycle. The first CO_2 formation peak under a CO-rich atmosphere showed a very sharp increase and a gradual decrease [Figs. 6(b) and 6(c)]. The increase was observed exactly at the same time as the amount of the adsorbed CO increased. The tail of the CO_2 peak showed similar behavior as the decrease of the CO gas concentration in the cell [Fig. 6(a)]. This indicates that the CO_2 was formed at once and the CO_2 concentration decreased according to the mixing property of the cell. The second peak under an O_2-rich atmosphere was initiated by a relatively slow CO_2 formation and followed by a sudden increase at the same time as the adsorbed CO decreased. The second CO_2 formation showed a long-tail behavior, which was clearly different from the one observed for CO gas [Fig. 6(a)], thus indicating that a simple mixing in the cell cannot be responsible for it. The long-tail behavior can be due to a continuously occurring reaction or a slow desorption of CO_2 from the surface. The clear difference between the two peaks indicates that the corresponding mechanisms of the CO_2 formations are different.

b. Past transient studies. CO oxidation over Pt has been widely studied by dosing or impinging CO over the oxygen-precovered surface mostly under UHV conditions to elucidate transient species during the reaction.[16,19,20,23–26,41] Some studies analyzed CO_2 formation[23,25] and others assumed fast formation and desorption of CO_2 from Pt surfaces.[19,24] The assumption of fast CO_2 desorption is reasonable when dosing CO over an oxygen-covered Pt surface due to the stronger adsorption of CO on Pt compared with CO_2 and oxygen.[17,22] However, the first CO_2 formation decreased significantly to nearly zero at the longer modulation period (Fig. 9), and the mechanisms proposed based on the studies using the order of O_2 adsorption followed by exposure to CO atmosphere are probably not relevant here. A few studies of transient types have dealt with the reverse order, i.e., change from CO to O_2 atmosphere.[14,21] A fluorescence yield near-edge spectroscopy (FYNES) study reported also a sudden drop in the amount of the adsorbed CO upon temperature increase and a mild drop with isothermal oxidation experiments both starting from a CO-covered Pt surface under O_2 atmosphere.[21] The study showed that the onset temperature for oxidation decreased with increasing oxygen pressure and that the desorption of CO is necessary for the initiation of the oxidation reaction.

The need to initially remove (by desorption or reaction) a certain amount of CO in order to promote fast reaction can be the reason for the observed induction period and may play an important role in our study. Yet the assumption of prompt gaseous CO_2 formation upon disappearance of adsorbed CO as well as the fact that CO_2 gas was not detected in the mentioned study make further comparisons to our study difficult.

A recent STM study shed some light on the reaction mechanism and the state of the Pt surface under high pressure by modulating CO and O_2 pressures, both 0.5 bar, at 425 K in a flow reactor similar to the one used in our study.[14,15] Two active phases were observed in an O_2-rich atmosphere; one phase where reaction occurs on Pt terraces with a low activity, and the other phase with a high activity where Pt oxide islands were formed on the Pt surface.

c. Origin of CO_2 formation under an O_2-rich atmosphere. When the time scale of the STM study is compared with our study, the activity jump of the second CO_2 formation falls into the low-activity phase. The CO_2 production of the low-activity phase in the reactor-STM was ca. 0.5 mbar, which is well within our detection limit. An estimate based on filling the cell with air (0.360 mbar CO_2 was assumed) and He (reference) gives an integrated signal of 1.0 abs cm^{-1} [Fig. 6(c)] for 0.368 mbar CO_2. However, the great difference of the residence time in the reactors must be properly taken into account. On the other hand, when CO concentration is compared with our study, the activity jump falls into the high-activity phase. Under 0.5 bar O_2 at 425 K, the threshold CO concentration value, below which the active Pt oxides are formed, was ca. 20 mbars, corresponding to 2.0% CO in our study. The CO concentration in our study was therefore below the threshold value during the jump in the second CO_2 formation. The O_2 concentration dependence of the induction period (Fig. 6) supports the viewpoint based on concentration. The 5% O_2 was high enough to produce the highly active phase of the Pt with some delay (induction time). The delay may be related more to the ratio between CO and O_2 concentrations than the absolute concentration of CO and O_2, thereby the dilution of CO is required to activate the surface under low O_2 pressures, resulting in the observed induction time. A similar interpretation was given by the authors of the STM study.[14] Usage of 1.25 bar O_2 lead to an increase of the CO threshold concentration to ca. 40 mbars, supporting that the CO/O_2 ratio is important for the active phase formation.[14]

Assuming the activity jump is the transition to the active Pt oxide phase, the gradual CO_2 formation before the jump [Fig. 6(c)] is most probably in the low-activity phase. The considerable amount of the adsorbed CO during the gradual formation agrees well with the observation that the Pt surface was not reconstructed in the low-activity phase and mainly covered by CO.[14] The dependence of the amount of the gaseous CO_2 on the O_2 concentration (Fig. 7) implies that more active oxide phases can be stabilized by the reaction mixture, especially under high concentrations of O_2.

d. Origin of CO_2 formation under a CO-rich atmosphere. The origin of the first CO_2 formation is discussed next. One obvious possible origin of the formation is the reaction of incoming CO with the active oxide. However, the experiments with long modulation periods showed nearly no first CO_2 formation. This could imply that the oxide is actually not active when the atmosphere is changed rapidly to CO and that the high concentration of CO reconstructs the oxide to a metallic Pt surface and immediately covers it. This CO, most likely coadsorbing with oxygen, was indicated by the high CO stretching frequency (Fig. 4).

The second possible origin of the first CO_2 formation is the desorption of the CO_2 precursor. The first scenario within this second possibility is that upon entering the high-activity phase the adsorbed CO reacts with oxygen, forming a CO_2 precursor on the surface, and then the precursor slowly desorbs. In this case, the amount of CO_2 will be determined by the amount of adsorbed CO in the metallic phase. This explains well the constant CO_2 formation observed at 433 K. A rough estimate of the amount of CO_2 formation from the Pt film [assuming all the CO_2 molecules are formed from the adsorbed CO, CO is adsorbed at atop position on all Pt atoms of Pt(111) surface, and the sample surface area is 1 cm^2] yields an instantaneous pressure of 8.8 μbars (6.9 ml of the reactor volume) and 20.3 μbars (3.0 ml of the reactor volume, to account only for the near-surface volume), which correspond to 0.024 and 0.055 abs cm^{-1} of Fig. 6(c), respectively. This is obviously far below the observed CO_2 amount, even when the surface roughness and a higher Pt surface area are taken into consideration. This is a clear proof that more than one turnover takes place during the first CO_2 formation and that CO molecules present in the O_2 atmosphere have reacted.

The second scenario of the second possibility is that CO adsorbs and reacts with oxygen to produce the adsorbed CO_2 precursor, which desorbs slowly. This possibility explains well all the observations of this study. When the gas is switched from CO to O_2, a small conversion of CO occurs during the low-activity phase and the conversion should be the same for all periods since the induction times are the same. Upon entering the high-activity phase, CO molecules present at low concentrations in the gas phase react with oxygen of the active surface, forming the CO_2 precursor without reconstructing back to the CO-adsorbed metallic Pt surface. Most likely, the CO_2 precursor desorbs slowly, causing the long-tail behavior of the second peak. The rates of the CO_2 precursor desorption and the consequent turnover of the reaction are most likely dependent on the CO concentration in the gas phase. When the modulation period is long, most of the precursor desorbs since all CO molecules in the gas phase have left the cell or have reacted, and no CO_2 precursor is produced on the surface. In contrast, when the period is short, the remaining nondesorbed precursors desorb readily due to the surface reconstruction induced by the concentrated CO atmosphere and the displacement by the strongly adsorbing CO. Within this possibility, a constant CO_2 formation is expected when the reactivity of the surface is high enough such that the absence of CO in the gas phase is reached during the high-activity phase. The increase in the CO_2 formation towards the longer periods at 373 and 403 K (Fig. 8) can be explained by the low activity of the surface and the smaller amount of the CO_2 precursor formation at shorter periods. Figure 6 shows that towards the end of the modulation period there is no CO, adsorbed and gas, visible in the spectra, whereas CO_2 is detected. An estimate was therefore made to clarify whether this is compatible with instantaneous conversion of CO to CO_2. The intensity of 1 mbar CO and CO_2 gives 0.12 and 2.72 abs cm^{-1}, respectively. This means more than 20 times higher sensitivity for CO_2 than for CO in the gas phase. When (i) the confident detection limit for CO_2 is set to 0.05 abs cm^{-1}, (ii) 100% instantaneous conversion from CO to CO_2 is assumed, and (iii) the sensitivity ratio between CO_2 and CO is considered then a mixing tank model, which sufficiently describes the mixing behavior of the gases in the cell,[31] predicts 58.7 s (most probably shorter due to the CO consumption by the reaction) as the time required to reach the CO concentration (0.38 μbar) that yields a CO_2 signal of 0.05 abs cm^{-1} at 60 ml/min flow rate

after the atmosphere is switched from CO to O_2. After 58.7 s in the second-half period (Fig. 6), CO_2 formation is considerably higher than the detection limit, disproving the instantaneous conversion from CO to CO_2 and supporting the presence of slowly desorbing CO_2 precursors.

The infrared spectra (950–4000 cm^{-1}) do not give evidence for a precursor with the expected behavior (i.e., increasing during the active phase and decreasing during desorption), which indicates that the CO_2 precursor is probably infrared inactive. The presence of the CO_2 precursor has been reported by a Cs^+ reactive ion scattering study,[22] although a direct comparison with our study is difficult due to the different conditions [order of atmosphere change (from O_2 to CO) and pressure difference]. The precursor can simply be horizontally adsorbed CO_2 on Pt oxide, thus being invisible in the infrared.

2. Baseline change

Based on the previous discussion, it is speculated that the step change of the baseline coinciding with the appearance and disappearance of the adsorbed CO (Fig. 3) is also due to oxide formation. Now the baseline change is further discussed in terms of the reflectivity change caused by the refractive index difference of the substrates, i.e., Pt and Pt oxide covered surface. The reference of the normalized ME PM-IRRAS spectra of the CO/O_2 modulation experiments was the last spectrum of the period and measured in the high-activity phase. When the surface is covered by CO and assumed as a metallic Pt phase, the baseline is expressed in terms of the bare substrates:

$$\left(\frac{\Delta R}{R}\right)_{\mathrm{norm,Pt}} = \frac{(\Delta R/R)_{\mathrm{Pt}}}{(\Delta R/R)_{\mathrm{AP}}} - 1, \tag{5}$$

where AP stands for the active phase. Obviously, the baseline of the active phase is zero. The observed baseline change Δb was between 0.002 and 0.01, and Δb can be expressed as the negative value of Eq. (5). By neglecting the $J_0(\varphi_0)$ term in Eq. (3) (assuming $R_p \simeq R_s$) and introducing the reflectance ratio ($\rho = R_p/R_s$), an experimental PM-IRRAS signal of a bare substrate can be written as

$$\left(\frac{\Delta R}{R}\right)_{\mathrm{sub}} = \frac{g \cdot |(\gamma R_p - R_s) \cdot J_2(\varphi_0)|}{\gamma R_p + R_s} = \frac{g \cdot |(\gamma\rho - 1) \cdot J_2(\varphi_0)|}{\gamma\rho + 1}. \tag{6}$$

The value of ρ is determined by experimental parameters such as the angle of incidence and also by material parameters such as complex reflective index $\tilde{n} = n - ik$, where n is the index of refraction and k is the extinction coefficient. The Fresnel equation[42] with assumptions [two-phase system, the gas-phase refractive index is 1, the index of the Pt film is equal to that of the bulk Pt $\tilde{n}_{\mathrm{Pt}} = 5.71 - 23.35i$ (at 1670 cm^{-1}) (Ref. 43)] and the experimental angle of incidence yield 0.8108 for ρ_{Pt} (ρ value of Pt). Then the range of the effective complex refractive index of the active phase $\tilde{n}_{\mathrm{AP}}$ can be estimated from ρ_{Pt}, Eqs. (5) and (6), Δb, the Fresnel equation upon calculating ρ_{AP}, and an assumption of $\gamma = 1$. Figure 10 shows the range of possible refractive indices of the active phase. The index change can be small or large in both n and k, but the index is certainly changed. This indicates a phase change, because such a baseline move during desorption of CO from the surface was not observed. Furthermore, the baseline is constant during the high-activity phase where surface species are changing dramatically by the reaction, which shows that such a change cannot be due to surface species.

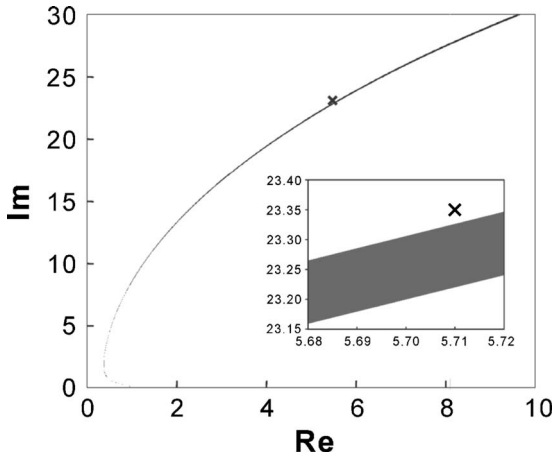

FIG. 10. Range of possible effective refractive index of the high-activity phase. Re and Im stand for the real and imaginary parts of the refractive index, respectively. The small window shows a zoomed view near the refractive index of bulk at 1670 cm^{-1} (shown as a cross point).

It is apparently not sufficient to determine the complex refractive index from the data applied in the analysis. A slight decrease in both real and imaginary parts of the refractive index can be anticipated as was seen in another wavelength region,[44] but the exact determination of the index requires other techniques, such as ellipsometry. Still, the determination is a big challenge with an appropriate method due to the influence of surface roughness on reflectivity,[45] and indeed a rougher surface is expected in the high-activity phase.[14]

3. Surface contamination

The presence and accumulation of surface species (950–1300 cm^{-1}) during the experiments were observed (Figs. 4 and 5). Judging from the absorbance in both figures, it is clear that the species at 1050 and 1230 cm^{-1} are not just continuously accumulating during the modulation experiments. The amount of these surface species increased upon CO adsorption or surface reconstruction to metallic Pt and decreased during the active phase. A small difference between the amount of formation and removal of the surface species probably resulted in the large accumulation during the numerous repeated cycles. The dissociation of adsorbed CO can be at the origin of the observed surface species. Although the dissociation of CO on Pt single crystals is found at higher temperatures (>500 K) than those of the current study, dissociation may be promoted due to the roughing of the surface by oxide formation. However, the kinetic behavior of the species was similar to that of the

adsorbed CO and therefore this species is not the surface CO_2 precursor and probably will not play an important role in the reaction.

V. CONCLUSIONS

A new technique based on PM-IRRAS utilizing reflectivity information, generally needed to calculate the surface spectrum in conventional use, was successfully applied to measure surface species, gas-phase species, and surface properties simultaneously during CO oxidation over Pt film under semirealistic conditions (high temperatures and pressures). The simultaneous measurement resulted in rich information and a rather complete picture on the reaction. The combination of modulation excitation spectroscopy with PM-IRRAS showed its potential for kinetic studies based on the analysis of responses of surface species and gas-phase species present near the surface. In addition, the technique leads to great enhancement of sensitivity due to averaging over several modulation periods and the phase-sensitive detection. The baseline move during the reaction could be explained by the change in the refractive index of near-surface bulk phase. Two reactive phases, low- and high-activity phases, were observed under an O_2-rich atmosphere. A large amount of atop CO was observed during the low-activity phase. Upon transition from low- to high-activity phase, the adsorbed CO completely disappeared and surface reconstruction from Pt to Pt oxide was indicated by the baseline step change. During the highly active phase in the O_2-rich atmosphere, the residual gaseous CO present near the surface reacted with the surface oxide to form a CO_2 precursor. A slow desorption of the CO_2 precursor in the O_2-rich atmosphere was indicated, but it desorbed at once when the gas phase was changed to a CO-rich atmosphere accompanying the surface reconstruction to the metallic Pt and a competitive adsorption of CO on the surface. The CO_2 precursor is most likely infrared inactive. In addition, accumulation of surface species was observed, which did not play an important role in the reaction. The results are in good agreement with recent high-pressure STM studies. The main potential of the technique applied in this study is that it provides information on adsorbed species, gas-phase species, and the near-surface solid phase simultaneously with good time resolution and high sensitivity. With these attractive features, it will be a valuable tool for investigations of various phenomena occurring at gas-solid interfaces.

ACKNOWLEDGMENT

We thank the Foundation Claude and Giuliana for financial support.

[1] S. A. Francis and A. H. Ellison, J. Opt. Soc. Am. **49**, 131 (1959); R. G. Greenler, J. Chem. Phys. **44**, 310 (1966).
[2] B. E. Hayden, in *Vibrational Spectroscopy of Molecules on Surfaces*, edited by J. T. Yates, Jr. and T. E. Madey (Plenum, New York, 1987).
[3] H. A. Pearce and N. Sheppard, Surf. Sci. **59**, 205 (1976).
[4] K. W. Hipps and G. A. Crosby, J. Phys. Chem. **83**, 555 (1979).
[5] W. G. Golden, D. S. Dunn, and J. Overend, J. Catal. **71**, 395 (1981).
[6] B. J. Barner, M. J. Green, E. I. Saez, and R. M. Corn, Anal. Chem. **63**, 55 (1991); M. J. Green, B. J. Barner, and R. M. Corn, Rev. Sci. Instrum. **62**, 1426 (1991).
[7] D. W. Goodman, J. Catal. **216**, 213 (2003).
[8] D. Blaudez, T. Buffeteau, J. C. Cornut, B. Desbat, N. Escafre, M. Pezolet, and J. M. Turlet, Appl. Spectrosc. **47**, 869 (1993); M. N. Islam and T. Kato, Langmuir **20**, 10872 (2004).
[9] H. Seki, K. Kunimatsu, and W. G. Golden, Appl. Spectrosc. **39**, 437 (1985); V. Zamlynny, I. Zawisza, and J. Lipkowski, Langmuir **19**, 132 (2003); K. Kunimatsu, H. Seki, W. G. Golden, J. G. Gordon, and M. R. Philpott, Surf. Sci. **158**, 596 (1985).
[10] V. A. Burrows, S. Sundaresan, and Y. J. Chabal, J. Vac. Sci. Technol. A **5**, 801 (1987).
[11] I. Langmuir, Trans. Faraday Soc. **17**, 621 (1922).
[12] R. Imbihl and G. Ertl, Chem. Rev. (Washington, D.C.) **95**, 697 (1995).
[13] P. W. Jacobs and G. A. Somorjai, J. Mol. Catal. A: Chem. **131**, 5 (1998); H. Over and M. Muhler, Prog. Surf. Sci. **72**, 3 (2003).
[14] B. L. M. Hendriksen and J. W. M. Frenken, Phys. Rev. Lett. **89**, 046101 (2002).
[15] B. L. M. Hendriksen, S. C. Bobaru, and J. W. M. Frenken, Catal. Today **105**, 234 (2005).
[16] J. Wintterlin, S. Volkening, T. V. W. Janssens, T. Zambelli, and G. Ertl, Science **278**, 1931 (1997).
[17] W. Li and B. Hammer, Chem. Phys. Lett. **409**, 1 (2005).
[18] C. T. Campbell, G. Ertl, H. Kuipers, and J. Segner, J. Chem. Phys. **73**, 5862 (1980); J. L. Gland and E. B. Kollin, *ibid.* **78**, 963 (1983).
[19] I. Nakai, H. Kondoh, K. Amemiya, M. Nagasaka, A. Nambu, T. Shimada, and T. Ohta, J. Chem. Phys. **121**, 5035 (2004); I. Nakai, H. Kondoh, K. Amemiya, M. Nagasaka, T. Shimada, R. Yokota, A. Nambu, and T. Ohta, *ibid.* **122**, 134709 (2005).
[20] M. Kinne, T. Fuhrmann, J. F. Zhu, C. M. Whelan, R. Denecke, and H. P. Steinruck, J. Chem. Phys. **120**, 7113 (2004).
[21] D. J. Burnett, A. T. Capitano, A. M. Gabelnick, A. L. Marsh, D. A. Fischer, and J. L. Gland, Surf. Sci. **564**, 29 (2004).
[22] S. J. Han, C. W. Lee, H. Yoon, and H. Kang, J. Chem. Phys. **116**, 2684 (2002).
[23] S. Hong and H. H. Richardson, J. Phys. Chem. **97**, 1258 (1993).
[24] J. H. Miners, P. Gardner, A. M. Bradshaw, and D. P. Woodruff, J. Phys. Chem. B **108**, 14270 (2004).
[25] M. D. Xu, J. Y. Liu, and F. Zaera, J. Chem. Phys. **104**, 8825 (1996).
[26] F. Zaera, J. Y. Liu, and M. D. Xu, J. Chem. Phys. **106**, 4204 (1997).
[27] Y. Iwasawa, R. Mason, M. Textor, and G. A. Somorjai, Chem. Phys. Lett. **44**, 468 (1976); K. McCrea, J. S. Parker, P. L. Chen, and G. Somorjai, Surf. Sci. **494**, 238 (2001); K. R. McCrea, J. S. Parker, and G. A. Somorjai, J. Phys. Chem. B **106**, 10854 (2002); X. C. Su, P. S. Cremer, Y. R. Shen, and G. A. Somorjai, J. Am. Chem. Soc. **119**, 3994 (1997); G. A. Somorjai, K. S. Hwang, and J. S. Parker, Top. Catal. **26**, 87 (2003); W. G. Roeterdink, J. F. M. Aarts, A. W. Kleyn, and M. Bonn, J. Phys. Chem. B **108**, 14491 (2004).
[28] T. Bürgi and A. Baiker, J. Phys. Chem. B **106**, 10649 (2002).
[29] D. Baurecht and U. P. Fringeli, Rev. Sci. Instrum. **72**, 3782 (2001).
[30] See EPAPS Document No. E-JCPSA6-124-703602 for the details of the ME PM-IRRAS cell design and ME PM-IRRA gas phase spectra of the CO/He modulation experiment. This document can be reached via a direct link in the online article's HTML reference section or via the EPAPS homepage (http://www.aip.org/pubservs/epaps.html).
[31] A. Urakawa, T. Bürgi, and A. Baiker (in press).
[32] M. Bieri and T. Bürgi, J. Phys. Chem. B **109**, 10243 (2005); R. Wirz, T. Bürgi, and A. Baiker, Langmuir **19**, 785 (2003); R. Wirz, T. Bürgi, W. Lindner, and A. Baiker, Anal. Chem. **76**, 5319 (2004).
[33] U. P. Fringeli, D. Baurecht, and H. H. Günthard, in *Infrared and Raman Spectroscopy of Biological Materials*, edited by H. U. Gremlich and B. Yan (Dekker, New York, 2000), p. 143.
[34] A. Urakawa, R. Wirz, T. Bürgi, and A. Baiker, J. Phys. Chem. B **107**, 13061 (2003).
[35] T. Buffeteau, B. Desbat, D. Blaudez, and J. M. Turlet, Appl. Spectrosc. **54**, 1646 (2000).
[36] T. Buffeteau, B. Desbat, and J. M. Turlet, Appl. Spectrosc. **45**, 380 (1991).
[37] X. C. Su, P. S. Cremer, Y. R. Shen, and G. A. Somorjai, Phys. Rev. Lett. **77**, 3858 (1996).
[38] G. Rupprechter, H. Unterhalt, M. Morkel, P. Galletto, T. Dellwig, and H. J. Freund, Vacuum **71**, 83 (2003).

[39] A. Crossley and D. A. King, Surf. Sci. **68**, 528 (1977).
[40] J. L. Gland and E. B. Kollin, Surf. Sci. **151**, 260 (1985).
[41] S. Volkening and J. Wintterlin, J. Chem. Phys. **114**, 6382 (2001).
[42] J. D. McIntyre and D. E. Aspnes, Surf. Sci. **24**, 417 (1971).
[43] T. Bürgi, Phys. Chem. Chem. Phys. **3**, 2124 (2001).
[44] Z. Y. Li, P. Beck, D. A. A. Ohlberg, D. R. Stewart, and R. S. Williams, Surf. Sci. **529**, 410 (2003).
[45] J. Caron and D. Jacquet, Appl. Spectrosc. **59**, 904 (2005).